Nuclear Engineering and Design 242 (2012) 19–25

Contents lists available at SciVerse ScienceDirect

Nuclear Engineering and Design

journal homepage: www.elsevier.com/locate/nucengdes

The various creep models for irradiation behavior of nuclear graphite

Xiang Fang[a], Haitao Wang[a], Suyuan Yu[a,*], Chenfeng Li[b]

[a] Institute of Nuclear and New Energy Technology, Tsinghua University, Beijing 100084, China
[b] Civil and Computational Engineering Centre College of Engineering, Swansea University, Swansea SA2 8PP, UK

ARTICLE INFO

Article history:
Received 9 May 2011
Received in revised form 7 September 2011
Accepted 14 September 2011

ABSTRACT

Graphite is a widely used material in nuclear reactors, especially in high temperature gascooled reactors (HTRs), in which it plays three main roles: moderator, reflector and structure material. Irradiation-induced creep has a significant impact on the behavior of nuclear graphite as graphite is used in high temperature and neutron irradiation environments. Thus the creep coefficient becomes a key factor in stress analysis and lifetime prediction of nuclear graphite. Numerous creep models have been established, including the visco-elastic model, UK model, and Kennedy model. A Fortran code based on user subroutines of MSC.MARC was developed in INET in order to perform three-dimensional finite element analysis of irradiation behavior of the graphite components for HTRs in 2008, and the creep model used is for the visco-elastic model only. Recently the code has been updated and can be applied to two other models—the UK model and the Kennedy model. In the present study, all three models were used for calculations in the temperature range of 280–450 °C and the results are contrasted. The associated constitutive law for the simulation of irradiated graphite covering properties, dimensional changes, and creep is also briefly reviewed in this paper. It is shown that the trends of stresses and life prediction of the three models are the same, but in most cases the Kennedy model gives the most conservative results while the UK model gives the least conservative results. Additionally, the influence of the creep strain ratio is limited, while the absence of primary creep strain leads to a great increase of failure probability.

1. Introduction

Graphite is the main structure material in high temperature gas-cooled reactors (HTRs), and it is also used for neutron moderators and reflectors in the reactor core. The structural integrity of the graphite components in the reactor core, along with the contributions of temperature, irradiation, and load, has a strong impact on the entire reactor's safety (Ishihara et al., 2004; Iyokua et al., 2004). When graphite components are subjected to non-uniform temperature and irradiation loads, the irradiation deformation and physical properties (such as strength, elastic modulus, coefficient of thermal expansion, creep factor and thermal conductivity) of graphite change, and stresses are generated and grow (Burchell and Snead, 2007; Engle and Kelly, 1984). High temperature fast neutron irradiation creep plays an important role in the whole process (Birch and Bacon, 1983; Blackstone, 1977). On one hand it can relieve the stresses and offset most of them; on the other hand it changes the dimensions of components, first in the form of shrinkage and later in the form of expansion. This can strongly influence the structural reliability and the service life of graphite components. A careful and comprehensive stress analysis and the corresponding life prediction based on three different creep models were carried out in order to ensure that the service life of graphite meets the design need.

The irradiation behavior of graphite has been studied for many years. Irradiation-induced creep strain is commonly considered to be made up of two parts: primary creep strain ε^{PC} and secondary creep strain ε^{SC}. ε^{PC} is approximated as σ/E_0, and ε^{SC} is expressed as $\varepsilon^{SC} = k\sigma\gamma$, where σ is stress, E_0 is the unirradiated Young's modulus, γ is neutron dose, and k is the secondary creep coefficient. There is already a series of irradiation creep constitutive models based on continuum mechanics to describe the secondary creep coefficient k under high temperature and irradiation conditions (Kelly and Burchell, 1994a; Oku and Ishihara, 2004), such as the linear visco-elastic model, the UKAEA model (Kelly and Brocklehurst, 1977) and the Kennedy model (Kennedy et al., 1980). These creep models are all based on continuum mechanics and come from the results of various irradiation tests when stressed graphite specimens are subjected to fast neutron fluence, and the predicted creep strain calculations agree well with experimental data. In order to evaluate the stresses and service life of graphite components, both the fast neutron and temperature distributions inside the reactor core are required as input data for irradiation-induced stress analysis. A significant amount of irradiated graphite data is required, including Young's modulus, coefficient of thermal expansion, irradiation strain, creep coefficient, and thermal conductivity,

* Corresponding author. Tel.: +86 10 62784824 412.
E-mail address: suyuan@tsinghua.edu.cn (S. Yu).

0029-5493/$ – see front matter © 2011 Elsevier B.V. All rights reserved.
doi:10.1016/j.nucengdes.2011.09.024

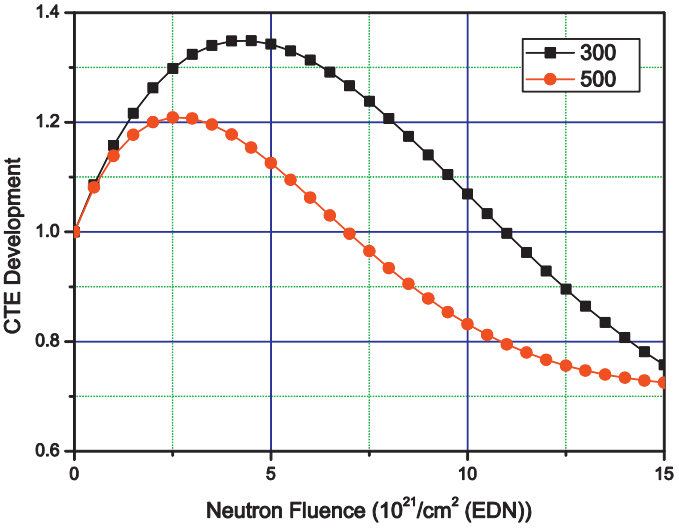

Fig. 1. CTE Development for ATR-2E at 300 °C and 500 °C.

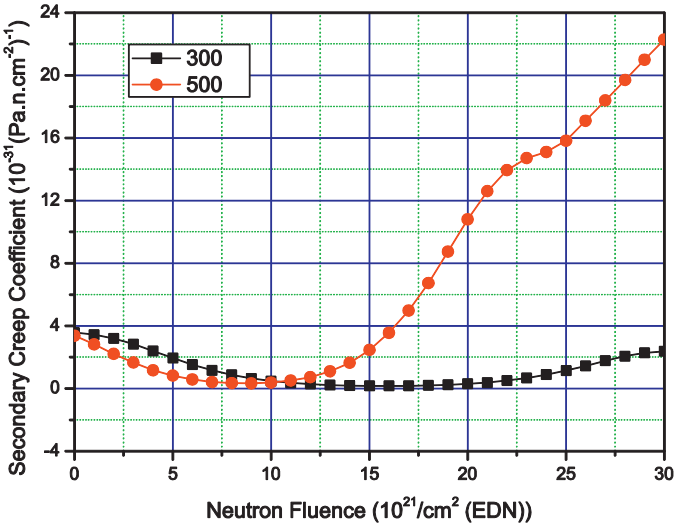

Fig. 2. Secondary creep coefficient development for ATR-2E at 300 °C and 500 °C.

etc. In the UKAEA model and Kennedy model, Young's modulus and dimensional changes are also used to calculate the secondary creep coefficient, making separate data for secondary creep coefficient unnecessary in these two models.

Based on the proposed creep models and experimental data, the finite element method (FEM) has been used to perform stress analysis and evaluation of graphite components (Berre et al., 2008; Tsang and Marsden, 2005). However, there are still some uncertainties in the creep models which could significantly affect the results of stresses analysis and lifetime evaluation. Two main uncertainties—the influence of the primary creep strain and the selection of the lateral creep strain ratio—have been studied and discussed. These uncertainties are taken into consideration in the analysis of graphite components (Kelly and Burchell, 1994b). The increase of the lateral creep strain ratio and absence of the primary creep strain will cause the visco-elastic model to predict increased stress levels and a shortened of service life (Wang and Yu, 2008). In order to achieve a more comprehensive model comparison and to ensure a more accurate assessment of the structural integrity of graphite components, the sensitivity analysis including the influence of the primary creep strain and the selection of creep strain ratio also needs to be applied to the other two models.

2. Irradiation performance of nuclear graphite

Numerous results of experiments and simulations of the behavior of nuclear graphite under high temperature and fast neutron irradiation have been published (Brennan and Kline, 1967; Henson et al., 1968; Jenkins and Stephen, 1966; Kelly, 1982, 1992; Matsuo and Saito, 1985a,b,c). The results show that nearly every parameter of graphite changes greatly with increased irradiation. Four parameters were reviewed: the coefficient of thermal expansion (CTE) α, the secondary creep coefficient k, Young's modulus E, and percentage volume change $\Delta V/V$. The CTE affects the thermal behavior of graphite significantly and directly, while the other three parameters are key factors for describing graphite creep behavior in the visco-elastic model, the UKAEA model and the Kennedy model.

CTE and its changing due to high temperature and irradiation have a major impact to the design of graphite components. To avoid excessively high thermal strain and stress caused by temperature changes, the thermal expansion behavior and related factors must be researched and summarized. CTE changes significantly with varieties of irradiation temperature and neutron dose. Fig. 1 shows experimental results of α/α_0 of extrusion molding nuclear graphite ATR-2E (made from special pitch coke) versus neutron dose at 300 °C and 500 °C (Haag, 2000). α_0 is the initial CTE of ATR-2E graphite without irradiation. It is clear that with increasing neutron dose, CTE increases initially, but decreased after reaching a maximum value. In 300 °C, both the value of CTE and the neutron dose at the maximum point are greater than that in 500 °C. The CTE data in Fig. 1 is used to calculate thermal strain in subsequent FEM calculations.

It is well known that creep exists when nuclear graphite under load is exposed to high temperature and fast neutron irradiation conditions. Moreover, the creep coefficient is also greatly affected by temperature and fast neutron fluence. The data of creep coefficients k is gained by calculation from constant load (5 MPa in both tensile and compressive load cases) irradiation creep tests carried out on small samples (Haag et al., 1987a,b). Fig. 2 shows the secondary creep coefficient curve of ATR-2E versus neutron dose at 300 °C and 500 °C. k remains constant after the initial irradiation, then decreases slightly and increases rapidly after the neutron dose rises to 1–1.5 × 10^{22} n cm^{-2} (EDN). k at 500 °C reaches 22 × 10^{-31} (Pa n cm^{-2})$^{-1}$ at a neutron dose of 3 × 10^{22} n cm^{-2} (EDN) and is eight times greater than that at 300 °C, which means a higher temperature greatly accelerates the rate at which k increases.

The reason the secondary creep coefficient trends this way is attributed to the change of the Young's modulus E at high temperature and high neutron fluence. Kelly and Brocklehurst's analysis of irradiation creep predicts that k should be proportional to C_{44}/E (Kelly and Brocklehurst, 1971), where C_{44} is the single crystal elastic constant for basal shear. The irradiation-induced change of the Young's modulus is divided into three components: one due to dislocation pinning (Kelly and Foreman, 1974), one due to structural changes and the last due to rapidly increasing porosity at high fluence (Burchell et al., 1986). In low neutron fluence dislocation pinning causes C_{44} and E to rise together to a plateau, with their ratio remaining constant. Later in irradiation, structural change causes a secondary increase in E without a concurrent change in C_{44}, which makes k decrease slightly. Oxidation causes a drastic fall of E in the final stage of irradiation (when the neutron fluence is up to 1–1.5 × 10^{22} n cm^{-2} (EDN)), which also results in the rapid increase of k. Fig. 3 shows the Young's modulus curves for ATR-2E versus neutron dose at 300 °C and 500 °C (Haag et al., 1990). The experimental curves for k and E show good qualitative agreement with Kelly and Brocklehurst's explanation.

High-temperature and fast neutron irradiation also lead to deformations of the graphite components due to dimensional

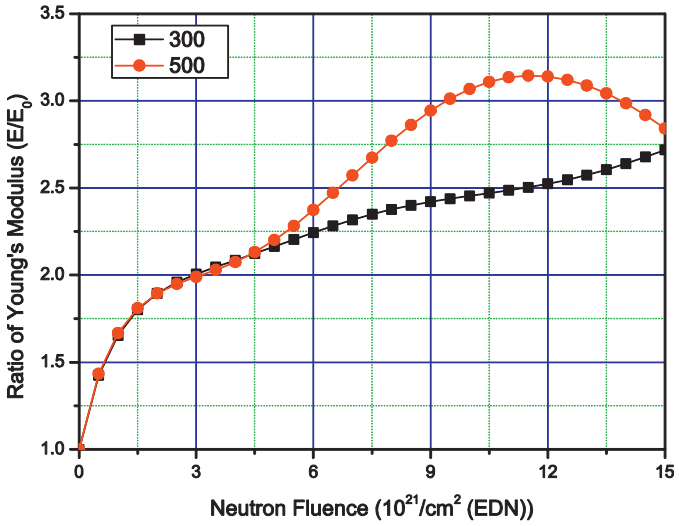

Fig. 3. Young's modulus development for ATR-2E at 300 °C and 500 °C.

changes, resulting in large stresses. The dimensional changes in graphite at temperatures of interest to HTRs exhibit shrinkage in the early stage, and as rapid expansion later (Kelly, 1991). The graphite components have not only thermal strain arising from non-uniform temperature distribution, but also irradiation shrinkage strain and creep strain due to fast neutron radiation exposure in the operational condition of the reactors; therefore the dimensional changes and internal stresses become greater over time. Thus, as the accumulative operational time increases, the deformations inside the graphite components become greater, and may lead to failure of the graphite bricks. The trend of irradiation percentage volume change of ATR-2E is shown in Fig. 4 (Haag et al., 1990). With the temperature rising from 300 °C to 750 °C, the initiation of shrinking and expanding occur earlier and graphite degrades much sooner.

3. Constitutive law and creep models

The constitutive relationship for nuclear graphite under temperature distributions and fast neutron irradiation:

$$\sigma = D\varepsilon^E = D(\varepsilon - \varepsilon^T - \varepsilon^R - \varepsilon^C), \tag{1}$$

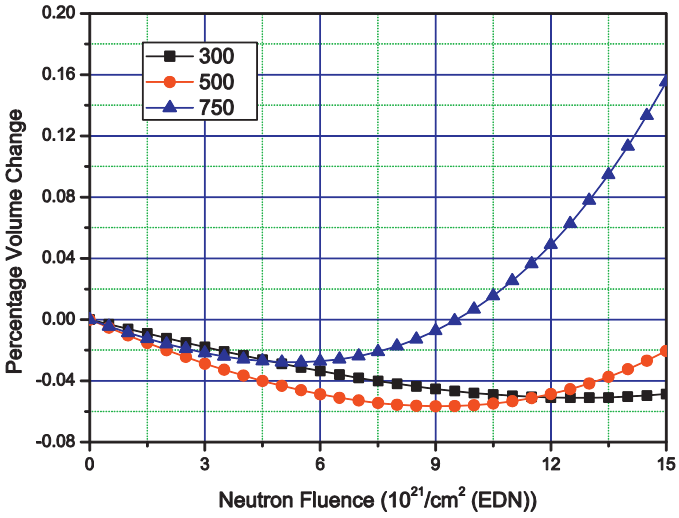

Fig. 4. Volume change for ATR-2E at 300 °C, 500 °C and 750 °C.

where σ is the stress tensor, and D is the elastic matrix, which is a function of temperature T and dose γ. ε is the total strain tensor consisting of elastic strain ε^E, thermal strain ε^T, irradiation-induced strain ε^R, and creep strain ε^C. The incremental form of ε^T is αdT. ε^R comes from experimental data. Eq. (1) can be rewritten into an incremental form,

$$d\sigma = D(d\varepsilon - d\varepsilon^T - d\varepsilon^R - d\varepsilon^C) + \varepsilon^E dD. \tag{2}$$

Eq. (2) is used as FEM constitutive law for each increment. The creep strain consists of primary creep strain ε^{PC} and secondary creep strain ε^{SC} as previously mentioned, and the former is approximately equal to the elastic strain, expressed as

$$\varepsilon^C = \varepsilon^{PC} + \varepsilon^{SC} = \frac{\sigma}{E_0} + k\sigma\gamma. \tag{3}$$

The form of constitutive law derives from real experimental data and the classical plastic creep theory (Yao et al., 2007). Some contrast has shown that Eq. (3) is reasonable and consistent with experimental stress-strain curve (Kelly and Brocklehurst, 1977). The focus in this paper of describing creep behavior is how to determine the secondary creep coefficient k. Different models use different methods for this issue.

3.1. The visco-elastic model

The experimental data for k as shown in Fig. 1 is used directly in the visco-elastic model and it is the most efficient way to achieve the objective. However, little data of k is gained and only a few kinds of graphite (including ATR-2E) can be calculated this way. Nevertheless, as the visco-elastic model is the most intuitive method to reflect the experimental results and has been used for decades, the results of other models are verified and assessed by comparing with the results of visco-elastic model.

3.2. The UKAEA model

As mentioned previously, the change of k can be considered as caused by the change of E. Thus the data of the Young's modulus can be used to gain ε^{SC} instead of k. The irradiation-induced change in the Young's modulus E/E_0 can be described as

$$\frac{E}{E_0} = \left(\frac{E}{E_0}\right)_P \times \left(\frac{E}{E_0}\right)_S. \tag{4}$$

P and S indicate the components of the Young's modulus change due to dislocation pinning and structural change respectively. $(E/E_0)_P$ reaches saturation after a low fluence and is assumed to remain unchanged thereafter. $(E/E_0)_S$ is therefore equal to E/E^*, where E^* is the plateau value of the Young's modulus when dislocation pinning is assumed to reach saturation (at about $1–3 \times 10^{21}$ n cm^{-2} (EDN) at different temperatures; see Fig. 3). The creep coefficient k at a fluence of γ should therefore be given by

$$k(\gamma) = k_P \left[\frac{E^*}{E(\gamma)}\right] = k_P S(\gamma)^{-1}, \tag{5}$$

where k_P is the creep coefficient in the plateau region, and S can be seen as a fluence-dependent structural factor. The creep strain is

$$\varepsilon^C = \varepsilon^{PC} + \varepsilon^{SC} = \frac{\sigma}{E_0} + k_P \int_0^\gamma \sigma \cdot S(\gamma)^{-1} d\gamma. \tag{6}$$

3.3. The Kennedy model

The Kennedy model uses a more intuitive parameter, the percentage volume change $\Delta V/V$, to describe the secondary creep coefficient k. Since the trend of volume change is exactly the same

Table 1
Parameters for three creep models.

Case number	1	2	3
Lateral creep strain ratio	Same as elastic	0.5	0.5
Primary creep	Included	Included	Excluded

as the trend of k (see Figs. 4 and 2), k can be written in the form of the percentage volume change. The numerical formula is,

$$k(\gamma) = k_P \left[1 - \mu \frac{(\Delta V/V)(\gamma)}{(\Delta V/V)_m}\right], \tag{7}$$

where k_P is the creep coefficient in the plateau region (the same as k_P in the UKAEA model), $(\Delta V/V)_m$ is the maximum volume shrinking of the graphite, and μ is the empirical constant, $\mu = 0.75$. $(\Delta V/V)$ is a function of neutron dose and temperature. The creep strain is

$$\varepsilon^C = \varepsilon^{PC} + \varepsilon^{SC} = \frac{\sigma}{E_0} + k_P \int_0^{\gamma} \sigma \left[1 - \mu \frac{(\Delta V/V)(\gamma)}{(\Delta V/V)_m}\right] d\gamma. \tag{8}$$

4. FEM calculation and results

The main object of FEM calculation is to test and compare the stress and life sensitivities to the parameters of each creep model. A code based on user subroutines of MSC.MARC was developed in INET in order to perform three-dimensional finite element analysis of the irradiation behavior of the graphite components for the HTRs, and the constitutive law of graphite in high temperature and irradiation conditions shown in Eq. (2) was applied. Through the solution of nonlinear equations, the development history of irradiation deformation and stress of the graphite structure in reactor was determined. Furthermore, the integrity of graphite structure could be predicted using these results. A modified equivalent stress σ_{eq} is used to evaluate service lives of graphite components by defining an admissible failure probability P_{ad} (Schubert et al., 1991):

$$\sigma_{eq} = \sqrt{\tilde{\sigma}_1^2 + \tilde{\sigma}_2^2 + \tilde{\sigma}_3^2 - 2\upsilon(\tilde{\sigma}_1\tilde{\sigma}_2 + \tilde{\sigma}_2\tilde{\sigma}_3 + \tilde{\sigma}_3\tilde{\sigma}_1)} \tag{9}$$

υ is Poisson's ratio, $\tilde{\sigma}_i$ ($i = 1, 2, 3$) are modified principal stresses which are defined as:

$$\tilde{\sigma}_i = \begin{cases} \sigma_i, & \sigma_i \geq 0 \\ \sigma_i \dfrac{\sigma_T}{\sigma_C}, & \sigma_i < 0 \end{cases} \tag{10}$$

σ_i ($i = 1, 2, 3$) are principal stresses, σ_T and σ_C are the tensile and compressive strength, respectively.

The lateral creep ratio and model selection were switched by specific parameters. Three cases examined are listed in Table 1, all of which were calculated using each of the creep models. The material considered in the stress analysis and evaluation was for nuclear graphite grade ATR-2E. A typical side reflector block of HTRs was modeled by using the three-dimensional finite element method. Fig. 5 shows a 1/4 model of a block with symmetric conditions taken into consideration. The block has two circular holes, one for the control rod, and the other for the helium path. The left side is near the reactor core while the right side neighbors the peripheral carbon bricks. The fixed temperature of the inner-core side is given as 450 °C, while the other side is 280 °C. The maximum fast neutron fluence at the inner edge of the block reaches up to 1×10^{22} n cm^{-2} (EDN) at the end of 30 years' service life (EOF), and decreases in a radial direction towards the outside, following an exponential law.

Fig. 6 shows the temperature distributions at EOF. A large temperature gradient occurs near the control rod hole; Fig. 7 shows the modified equivalent stress distributions at EOF in case 1 using the visco-elastic model. The stress is concentrated in two areas in every case, and the main points P_1 and P_2 were chosen from them respectively.

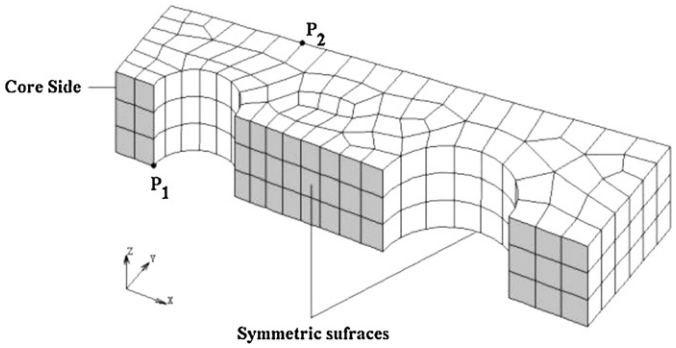

Fig. 5. Quarter model of side reflector component.

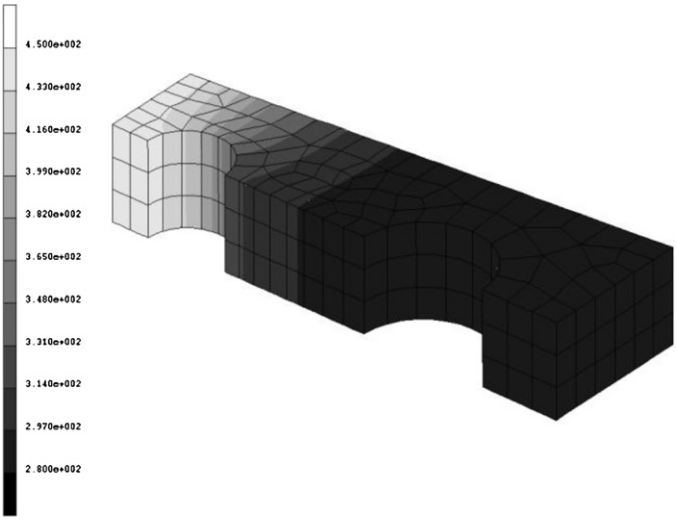

Fig. 6. Temperature distribution at EOF (unit: °C).

The curves of P_1's modified equivalent stresses are shown in Fig. 8. The stresses slightly increase then decrease in the first 20 years, and rise rapidly thereafter. The maximum value of each curve is at EOF, and reaches about 5–6 Mpa. The trends of case 1 and case 2 are different although they reach similar peak values.

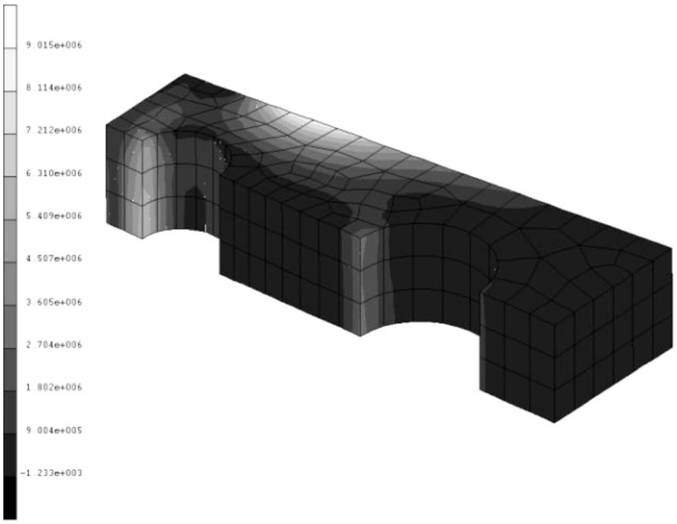

Fig. 7. Stress distribution at EOF in case 1 using the visco-elastic model (unit: Pa).

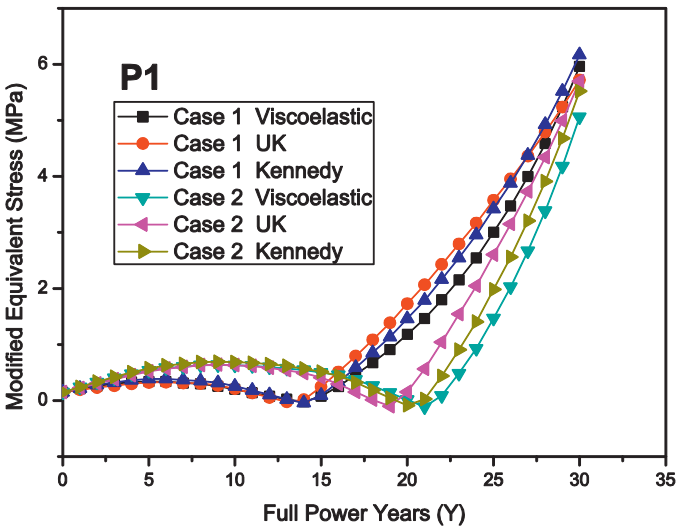

Fig. 8. Stress development at P_1: comparison.

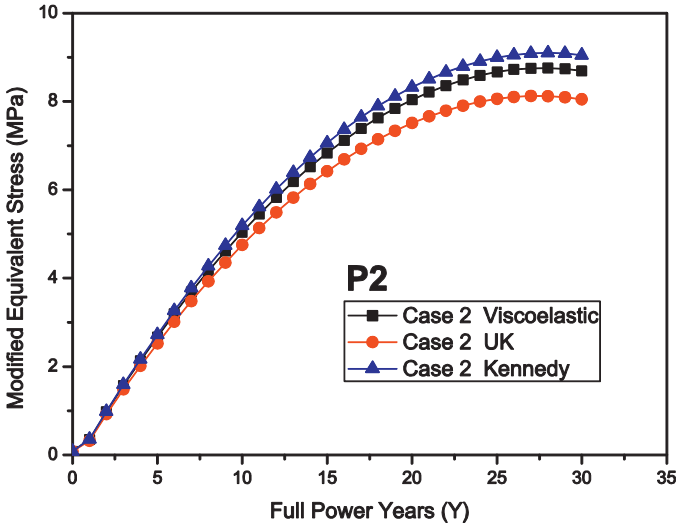

Fig. 10. Stress development at P_2 in case 2 using various models: comparison.

The stresses of case 1 reach the lowest point faster. However, for each case, the different models have identical stress trends, with negligible differences in their EOF values.

Figs. 9 and 10 show the modified equivalent stresses at P_2. The results of the two cases are too close to be easily distinguished from each other in the figures, which implies that the choice of creep ratio affects the stress at P_2 little in the selected temperature and irradiation range. The stresses increase continually throughout the lifetime of the graphite component, except at the end of its life. The peak values are reached near EOF, and reach about 8–9 MPa. Furthermore, the three models still give close results with variations of about 10%. The Kennedy model gives the highest stress, while the UKAEA model gives the lowest.

The results for structural integrity and life sensitivities are given in the form of corresponding failure probability as shown in Figs. 11–14. Under operation conditions, the failure probabilities in case 1 and case 2 are very close, just as the stresses at P_2. The peak value is about 10^{-7}. But the failure probability for case 3 is much higher and reaches 10^{-6} over a lifespan of 20 years, with a rapid increase near the end of the reactor's service life. This indicates the primary creep may affect the failure probability although it is low in value. Moreover, for each case, the Kennedy model always gives the

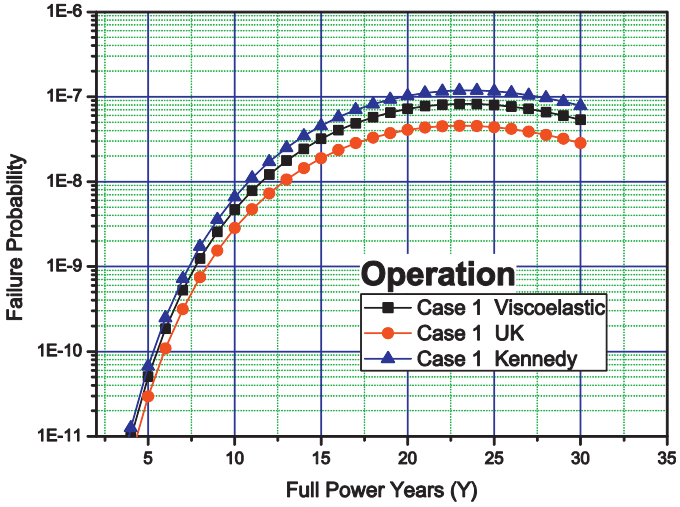

Fig. 11. Operation failure probabilities in case 1 using various models: comparison.

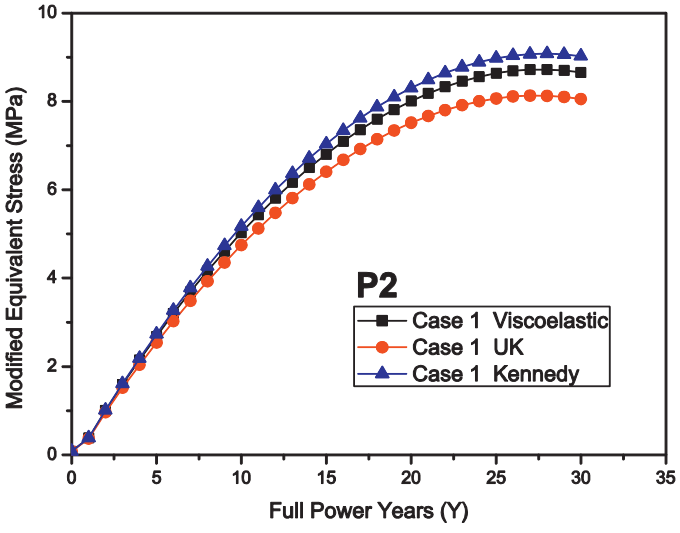

Fig. 9. Stress development at P_2 in case 1 using various models: comparison.

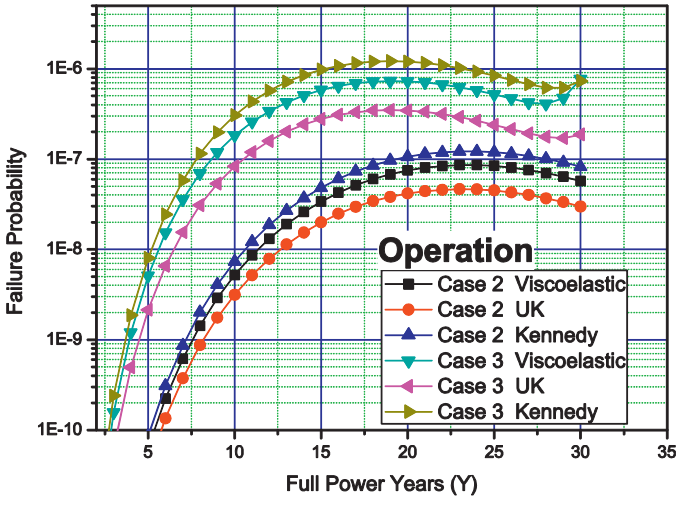

Fig. 12. Operation failure probabilities in cases 2 and 3 using various models: comparison.

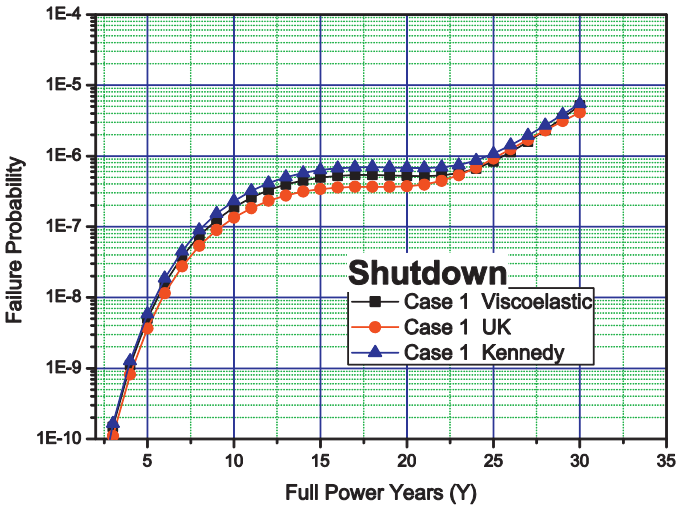

Fig. 13. Shutdown failure probabilities in case 1 using various models: comparison.

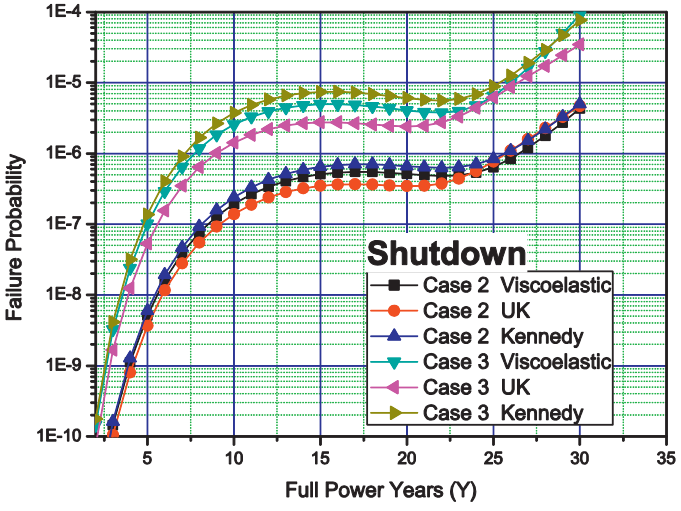

Fig. 14. Shutdown failure probabilities in cases 2 and 3 using various models: comparison.

most conservative results while the UKAEA model gives the most optimistic results.

Under shutdown conditions shown in Figs. 13 and 14, the failure probabilities are much higher with a rapid increase near EOF. The peak value for case 1 and case 2 is above and below 5×10^{-6} at EOF. For case 3, the failure probably is greater, reaching 0.9×10^{-4} using the visco-elastic model. The comparison of the different models shows less obvious differences for the shutdown failure probability value than for the operation failure probability value. Even so, the shape of different model's curves in each case is exactly the same.

5. Conclusions

Since nuclear graphite plays an important role as a moderator, reflector and main structure material in HTRs, its irradiation structure reliability is critical for operational safety. High temperature fast neutron irradiation creep which greatly affects the behavior of nuclear graphite exists throughout the whole process. Unfortunately experimental creep data are very limited, but numerous empirical based creep models based on continuum mechanics have been developed over several decades. In this study, three models, the visco-elastic model, UKAEA model, and Kennedy model have been programmed in a FEM code based on user subroutines of MSC.MARC by INET. Graphite behavior in the temperature range of 280–450 °C and for 30 years of service life (with fast neutron fluence reaching 1×10^{22} n cm^{-2} (EDN) at EOF) were simulated for all three models, and the numerical results were summarized. Additionally, some uncertainties—the influence of the primary creep strain and the selection of the lateral creep strain ratio have also been investigated.

Good agreements were also obtained with the results of all models, with about 10% difference among them. This indicates that any of the three models can be used to simulate graphite behavior and design graphite components. The Kennedy model usually gives the highest stress level and failure probability, and the results are the most conservative. In contrast, the UKAEA model always gives the lowest stresses and the results are the most optimistic. The selection of the secondary lateral creep ratio has little effect on the peak values of all curves, while the absence of primary creep may considerably decrease the service life of graphite components analyzed in this paper.

Acknowledgement

Financial supports for the project from the IAEA's Coordinated Research Project, the National Natural Science Foundation of China, under grant No. 10602029 and Research Fund for the Doctoral Program under grant No. 041588008 are gratefully acknowledged. The authors would also like to thank the Royal Academy of Engineering, for its support through the Research Exchanges with China and India Award.

References

Berre, C., Fok, S.L., Marsden, B.J., Mummery, P.M., Marrow, T.J., Neighbour, G.B., 2008. Microstructural modelling of nuclear graphite using multi-phase models. J. Nucl. Mater. 380 (1–3), 46–58.
Birch, M., Bacon, D.J., 1983. The effect of fast-neutron irradiation on the compressive stress–strain relationships of graphite. Carbon 21 (5), 491–496.
Blackstone, R., 1977. Radiation creep of graphite: An introduction. J. Nucl. Mater. 65, 72–78.
Brennan, J.J., Kline, D.E., 1967. Effect of low-dose reactor radiation on dynamic mechanical behavior of pyrolytic graphite. Carbon 5 (2), 181–188.
Burchell, T.D., Pickup, I.M., McEnaney, B., Cooke, R.G., 1986. The relationship between microstructure and the reduction of elastic modulus in thermally and radiolytically corroded nuclear graphites. Carbon 24 (5), 545–549.
Burchell, T.D., Snead, L.L., 2007. The effect of neutron irradiation damage on the properties of grade NBG-10 graphite. J. Nucl. Mater. 371 (1–3), 18–27.
Engle, G.B., Kelly, B.T., 1984. Radiation damage of graphite in fission and fusion reactor systems. J. Nucl. Mater. 122 (1–3), 122–129.
Haag, G., Delle, W., Nickel, H., Theymann, W., Wilhelmi, G., 1987. Development and testing of nuclear graphites for the German pebble-bed high temperature reactor. In: IAEA Specialists' Meeting on Graphite Component Structural Design. Summary Report (JAERI-M 86-192). Jaeri, Tokai, Ibaraki, Japan.
Haag, G., Delle, W., Kirch, N., Nickel, H., Reinhart, K., Ziermann, E.,1987b. Results of the visual in-pile inspection of the inner graphite reflector of the AVR. In: IAEA Specialists' Meeting on Graphite Component Structural Design. Summary Report (JAERI-M 86-192). Jaeri, Tokai, Ibaraki, Japan.
Haag, G., Mindermann, D., Wilhelmi, G., Persicke, H., Ulsamer, W., 1990. Development of reactor graphite. J. Nucl. Mater. 171 (1), 41–48.
Haag, G., 2000. Irradiation-induced creep in graphite and use of creep data in reactor design. In: 1st International Nuclear Graphite Specialists Meeting (INGSM), Oak Ridge, Tenn., USA, September.
Henson, R.W., Perks, A.J., Simmons, J.H.W., 1968. Lattice parameter and dimensional changes in graphite irradiated between 300 and 1350 °C. Carbon 6 (6), 789–806.
Ishihara, M., Sumita, J., Shibata, T., Iyoku, T., Oku, T., 2004. Principle design and data of graphite components. Nucl. Eng. Des. 233 (1–3), 160–251.
Iyokua, T., Ueta, S., Sumita, J., Umeda, M., Ishihara, M., 2004. Design of core components. Nucl. Eng. Des. 233 (1–3), 71–79.
Jenkins, G.M., Stephen, D.R., 1966. The temperature dependence of the irradiation induced creep of graphite. Carbon 4 (1), 67–72.
Kelly, B.T., Brocklehurst, J.E.,1971. Analysis of irradiation creep in reactor graphite. In: Proc. Third Conference on Industrial Carbons and Graphite. Society of Chemical Industry, London, p. 363.
Kelly, B.T., Foreman, A.J.E., 1974. Theory of irradiation creep in reactor graphite—dislocation pinning–unpinning model. Carbon 12 (2), 151–158.
Kelly, B.T., Brocklehurst, J.E., 1977. UKAEA reactor group studies of irradiation induced creep in graphite. J. Nucl. Mater. 65 (1), 79–85.
Kelly, B.T., 1982. Graphite—the most fascinating nuclear material. Carbon 20 (1), 2–11.

Kelly, B.T., 1991. The thermal expansion coefficients of graphite crystals—the theoretical model and comparison with 1990 data. Carbon 29 (6), 721–724.
Kelly, B.T., 1992. Irradiation creep in graphite—some new considerations and observations. Carbon 30 (3), 379–383.
Kelly, B.T., Burchell, T.D., 1994a. The analysis of irradiation creep experiments on nuclear reactor graphite. Carbon 32 (1), 119–125.
Kelly, B.T., Burchell, T.D., 1994b. Structure-related property changes in polycrystalline graphite under neutron irradiation. Carbon 32 (3), 499–505.
Kennedy, C.R., Eatherly, W.P., Senn, R.L., 1980. Compressive creep characteristics of graphite under irradiation. In: 33rd Pacific Coast Regional Meeting of the American Ceramic Society, San Francisco, October 26–29.
Matsuo, H., Saito, T., 1985a. Irradiation behaviors of nuclear grade graphite in commercial reactor (I) dimensional change and thermal-expansion. J. Nucl. Sci. Technol. 22 (2), 139–146.
Matsuo, H., Saito, T., 1985b. Irradiation behaviors of nuclear grade graphite in commercial reactor (II) thermal and physical-properties. J. Nucl. Sci. Technol. 22 (3), 225–232.
Matsuo, H., Saito, T., 1985c. Irradiation behaviors of nuclear grade graphite in commercial reactor (III) mechanical-properties. J. Nucl. Sci. Technol. 22 (4), 313–319.
Oku, T., Ishihara, M., 2004. Lifetime evaluation of graphite components for HTGRs. Nucl. Eng. Des. 227 (2), 209–217.
Schubert, F., Nickel, H., Breitbach, G., 1991. Structural design criteria for HTR-a summary report. Nucl. Eng. Des. 132, 75–84.
Tsang, D.K.L., Marsden, B.J., 2005. A mathematical stress analysis model for isotropic nuclear graphite under irradiation condition. J. Appl. Math. Mech. 4, 1–19.
Wang, H.T., Yu, S.Y., 2008. Uncertainties of creep model in stress analysis and life prediction of graphite component. Nucl. Eng. Des. 238 (9), 2256–2260.
Yao, H.T., et al., 2007. A review of creep analysis and design under multi-axial stress states. Nucl. Eng. Des. 237 (18), 1969–1986.